Detection and characterization of ZnO nanoparticles in surface and waste waters using single particle ICPMS

Madjid Hadioui[¥], *Vladimir Merdzan*[¥] *and Kevin J. Wilkinson**

[¥]These authors contributed equally to this paper

*kj.wilkinson@umontreal.ca; ORCID: 0000-0002-7182-3624

Accepted for publication in *Environ. Sci. Technol.* 2015, 49: 6141–6148; DOI: 10.1021/acs.est.5b00681

Department of Chemistry, University of Montreal, C.P. 6128, Succ. Centre-Ville, Montréal, QC H3C 3J7 Canada.

KEYWORDS. Zinc oxide, Single Particle ICPMS, Ion-Exchange, surface water, wastewater, metal nanoparticles.

TOC:

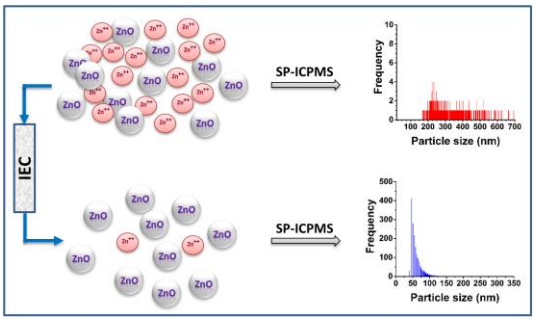

ABSTRACT

The increasing production of ZnO nanoparticles (nZnO) makes their analysis and characterisation extremely important from an ecological risk perspective, especially at the low concentrations at which they are expected to be found in natural waters. Single particle ICPMS (SP-ICPMS) is one of the few techniques available to detect and characterize nanoparticles at environmentally relevant concentrations. Unfortunately, at the very low particle concentrations where SP-ICPMS is performed, significant dissolution of the nZnO generally increases background levels of dissolved Zn to the point where measurements are not generally possible. By hyphenating SP-ICPMS with an ion-exchange resin, it was possible to characterize and quantify nZnO in order to gain insight into the nature of the nZnO in natural waters. Spiked and unspiked water samples were analysed using a SP-ICPMS that was coupled to a column containing a strong metal binding resin (Chelex 100). In addition to the detection of ZnO nanoparticles and the determination of its size distribution in natural waters, it was possible to partition the dissolved Zn among free and/or labile and strongly bound Zn fractions. In two natural waters, a high proportion (ca. 93 – 100%) of dissolved Zn was measured and the residual ZnO particles were mainly composed of small agglomerates (average sizes ranging from 133.6 to 172.4 nm in the surface water and from 167.6 to 216.4 nm in the wastewater effluent). Small numbers of small nanoparticles were also detected in non-spiked waters.

INTRODUCTION

In order to understand the fate and risk of nanomaterials (NM) in the environment, it is essential to accurately characterize their size, dissolution and agglomeration[1]. In natural systems, fate determinations of the inorganic NM are difficult due to their low concentrations and the simultaneous presence of other ionic and colloidal forms of the same elements. Indeed, toxicity or environmental fate data are often misinterpreted due to physicochemical transformations (e.g. agglomeration, dissolution, interactions with solid phases) of the NM[1] that have been unaccounted for in the experimental design.

Metal and metal oxide nanoparticles such as Ag, ZnO, TiO_2 and CeO_2 are among the most used nanomaterials in industrial and consumer products. This has led to increased attention in assessing their fate and behavior in the environment, especially in aquatic systems. ZnO nanoparticles (nZnO) are widely used in commercial products (sunscreens[2, 3], food additives, pigments, etc.) due to their high photo-reactivity, UV-blocking properties and medicinal uses[4-6]. The risk accompanying their widespread use, including their potential release into the environment, has led to numerous studies on their toxicity[7-14] as well as determinations of their aggregation and dissolution[15-17]. In almost all published investigations, relatively high concentrations of ZnO (>ppm levels) were considered even though low (<ppb) levels are predicted to occur in the environment. Unfortunately, few analytical techniques are available for detecting or characterizing low levels of nZnO in environmental (including toxicological) media. From this point of view, inductively coupled plasma mass spectrometry in its single particle mode (SP-ICPMS) is a promising technique for determining size distributions, particle mass and number concentrations and the dissolution of the inorganic nanomaterials[18-23]. To date, the technique has been mainly used for the characterization of gold[24-26] and silver[22, 27-29] nanoparticles; little success has been

achieved for highly soluble particles, such as nZnO[30]. A major difficulty arises when the concentration of dissolved metal is too high, in which case, the signal corresponding to the dissolved ions overlaps with that from the nanoparticles, leading to an erroneous (if not impossible) discrimination between the forms[31]. By coupling an ion-exchange column (IEC) with the SP-ICPMS (IEC-SP-ICPMS)[31], it is possible to remove much of the dissolved metal prior to data acquisition, thereby reducing the particle size detection limits of the technique and providing some information on the nature of the inorganic species in complex matrices. The objective of this work was thus to investigate the effectiveness of the IEC coupling and to apply the novel technique to the determination of nZnO fate in a surface and waste waters.

EXPERIMENTAL SECTION

Chemicals. High purity, ultrapure nitric acid (65%, Aristar Ultra) was purchased from BDH and used at a concentration of 1.5 M for the regeneration of the ion exchange resin. Sodium hydroxide (≥ 98%, Sigma-Aldrich) was used to convert the resin to its sodium form. ACS reagent grade $Ca(NO_3)_2$ and KCl were purchased from Sigma-Aldrich; $NaNO_3$ and NaCl (>99%) were obtained from Fisher Scientific and $Mg(NO_3)_2$ (>99%) was provided by Fluka. Zn calibration solutions were prepared by dilution of ICPMS standards (CGZN1-1, Inorganic Ventures). Suspensions of zinc oxide nanoparticles (Nanotek ZN-2551, nominal particle size of 50 nm, Alfa Aesar, Stock # 45588, Lot # L04U027) were prepared from a commercially obtained colloidal dispersion (50% w/w in H_2O). The average particle size provided by the manufacturer was obtained by transmission electron microscopy (TEM) performed on the dry powder. Prior to use, the nZnO dispersion was placed in an ultrasonic bath containing small pieces of ice, for 10 minutes. Particles were first diluted to 10 mg L^{-1} in ultrapure water (Milli-Q, 18.2 MΩ cm; total organic carbon < 2 µg L^{-1}) and

79 then spiked into the natural waters. With the exception of the kinetics studies, nZnO samples were
80 equilibrated for at least 24 hours prior to analysis. Fifty mg L^{-1} of citrate stabilized gold
81 nanoparticles with a nominal diameter of 60 nm (NIST reference material, RM 8013) was used to
82 determine the transport efficiency of the ICPMS.

83 **Ion exchange columns.** When analyzing samples, SP-ICPMS data were acquired with and without
84 the passage of sample through a cation exchange column, which was placed on line between the
85 peristaltic pump and the ICPMS nebuliser. The length of tubing between the exit of the column
86 and the entrance to the nebulizer was approximately 5 cm. An analytical grade Chelex 100 (50-
87 100 mesh, Sigma-Aldrich), with a binding capacity of 0.7 meq mL^{-1}, was used as the cation
88 exchange resin. Prior to use, the Chelex 100 resin was first washed with 1.5 M HNO_3, rinsed with
89 Milli-Q water and converted to its Na^+ form using 0.1 M NaOH, followed by a rinse with Milli-Q
90 water. The wet and swollen resin was then placed in a cut polypropylene tube with a length of 7.4
91 cm and an inner diameter of 2.8 mm. A resin bed volume of ca. 0.45 mL was maintained in the
92 column between two small pieces of glass wool, each retained by the cut top of a syringe. In a
93 limited number of experiments, an Amberlite®XAD1180N resin (20-60 mesh, moisture holding
94 capacity 61-67 %, 1.4 mL g^{-1} pore volume; Fluka) was used in a column with a length of 8.5 cm
95 and an inner diameter of 8.0 mm. In that case, due to the larger resin grain size, a wider column
96 was used to obtain better packing. Before use, 0.075 M HNO_3 and reagent grade ethanol (99%)
97 were used to condition the XAD1180N. Both resins were washed with Milli-Q water after every
98 second sample and data were acquired both to check for memory effects and to ensure that no
99 particles remained trapped in the interstitial volume of the column.

100 **Data acquisition and processing.** A Perkin-Elmer NexION 300x Inductively Coupled Plasma
101 Mass Spectrometer was used for data acquisition in single particle mode. The sample introduction

system consisted of a quartz cyclonic spray chamber, type C0.5 concentric glass nebulizer and quartz 2 mm bore injector. Time resolved signals were acquired in fast scan mode[32] using the Syngistix nano application module integrated into the NexION software (version 1.6 Build 1.6.4242.0). For verification purposes, raw data were also manually reprocessed (using Excel) as described previously[31]. Particles were discriminated from the background signal using a 3σ methodology (Syngistix module) or a value of σ=3 to 5 during the manual processing. All concentrations and diameters were determined from triplicate samples using 3 to 7 replicate measurements and a sample intake of 0.5 mL min^{-1}. Uncertainty values given in the paper represent standard deviations determined from the replicate measurements. For each measurement, 99000 data points were collected over 50 s using a dwell time of 0.5 ms and a negligible settling time (in the software, data are sent in packages of 1000 data points). Where relevant, representative intensity plots have been presented in the paper.

Particle number concentrations were determined from the number of events (detected particles), and a knowledge of the transport efficiency. Successive partial intensities were integrated into single particle events and the intensity of each event was converted to the equivalent mass of Zn using a calibration with ionic Zn standards. Particle diameters were determined from the known density of ZnO, the mass fraction of Zn/ZnO and by assuming spherical shape. Particle mass concentrations were obtained by summing the masses of all of the individual particles. The concentration of dissolved zinc was obtained by subtracting the concentration due to nanoparticles from the total Zn concentration. The concentration of dissolved Zn that was measured after passing the samples through the resins was attributed to strongly bound zinc. Free and/or labile Zn was obtained by subtracting the strongly bound Zn from the total dissolved Zn.

RESULTS AND DISCUSSION

SP-ICPMS (without resin). Suspensions of nZnO were diluted to sub-ppb (μg L^{-1}) levels (of total Zn), left for 24 hours (based upon the kinetic study showed in Figure S1) and analyzed by SP-ICPMS without the ion exchange resins. Based upon the presence of spikes in the time resolved signal (Figure 1), it was possible to conclude that nZnO was present; however dissolved Zn was very high (as demonstrated by the continuous background signal that increased with increasing nZnO concentrations from 1a to 1d). At the lowest nZnO concentrations (Figures 1a, 1b), particle numbers were too small to be statistically significant, while at higher concentrations (i.e. >10 μg L^{-1}; Figure 1c, 1d), background levels were so high that the signal for the dissolved Zn overlapped with that for the (smallest) nZnO. This is consistent with previous results for nAg showing that the minimal detectable particle sizes determined by SP-ICPMS increased with increasing dissolved metal[31]. Under these conditions, only very large particles or particle agglomerates can be distinguished from the dissolved Zn. Such a result is consistent with high nZnO dissolution, a result that has been consistently observed in the literature (e.g. [10, 14]), especially at lower particle concentrations[33]. Indeed, for a polyacrylic acid coated nZnO, Merdzan et al.[33] used centrifugal ultrafiltration to show that dissolution was much greater at low concentrations as opposed to high ones (i.e. 90% dissolution at 70 μg L^{-1} Zn and 30% dissolution at 1120 μg L^{-1} Zn). Similarly, Miao et al.[10] have reported greater release of Zn^{2+} for nZnO concentrations below 7.8 mg L^{-1}. In that case, Zn release decreased with time and was no longer significant after 4 days.

143

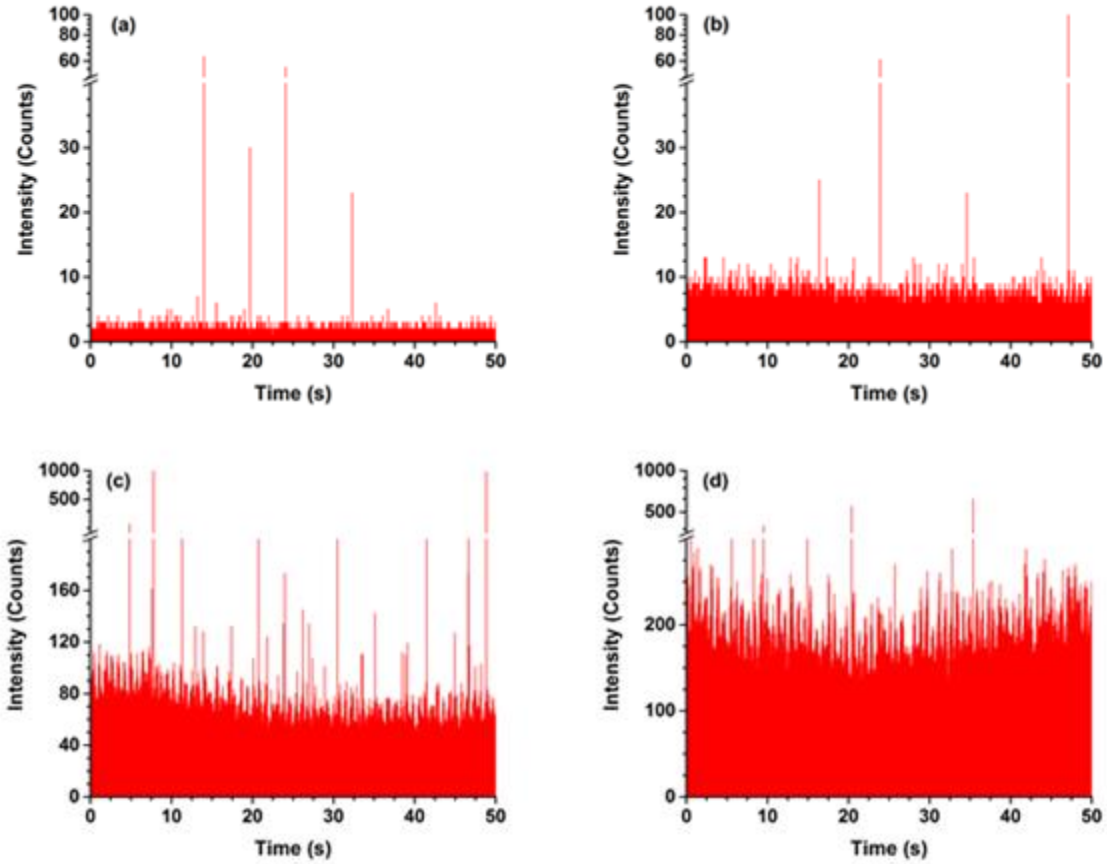

144

145 **Figure 1.** Raw intensity plot of a suspension of ZnO nanoparticles with a nominal diameter (as
146 provided by the manufacturer) of 50 nm in MilliQ water. Zn concentrations were equal to: (a)
147 0.07 µg L^{-1}, (b) 0.94 µg L^{-1}, (c) 17.74 µg L^{-1} and (d) 52.12 µg L^{-1}.

148

149 **IEC-ICPMS.** By coupling the SP-ICPMS to a Chelex 100 resin, it was possible to decrease the
150 background signal due to dissolved Zn, leading to a particle size distribution (Figures 2c, 2d) that
151 was more consistent with information provided by the manufacturer. As observed previously for
152 nAg[31], the use of the IEC resin did not appear to retain a significant proportion of the ZnO
153 nanoparticles (Figure S2). For a suspension initially composed of 51.5 µg L^{-1} nZnO in MilliQ
154 water, an average particle size of 65.4 ± 0.5 nm with a mode at 49.3 ± 2.2 nm was obtained using

IEC-SP-ICPMS whereas, in the absence of resin, only a few events of high intensity (average diameter of ca. 205 nm) could be distinguished from the dissolved Zn. Similarly, for a lower concentration of 17.7 µg L^{-1} Zn in MilliQ water, an average particle diameter of 67.3 ± 6.2 nm (mode: 45.6 ± 7.7 nm) was obtained (mean of 151.6 nm and mode of 143.3 nm were determined using SP-ICPMS).

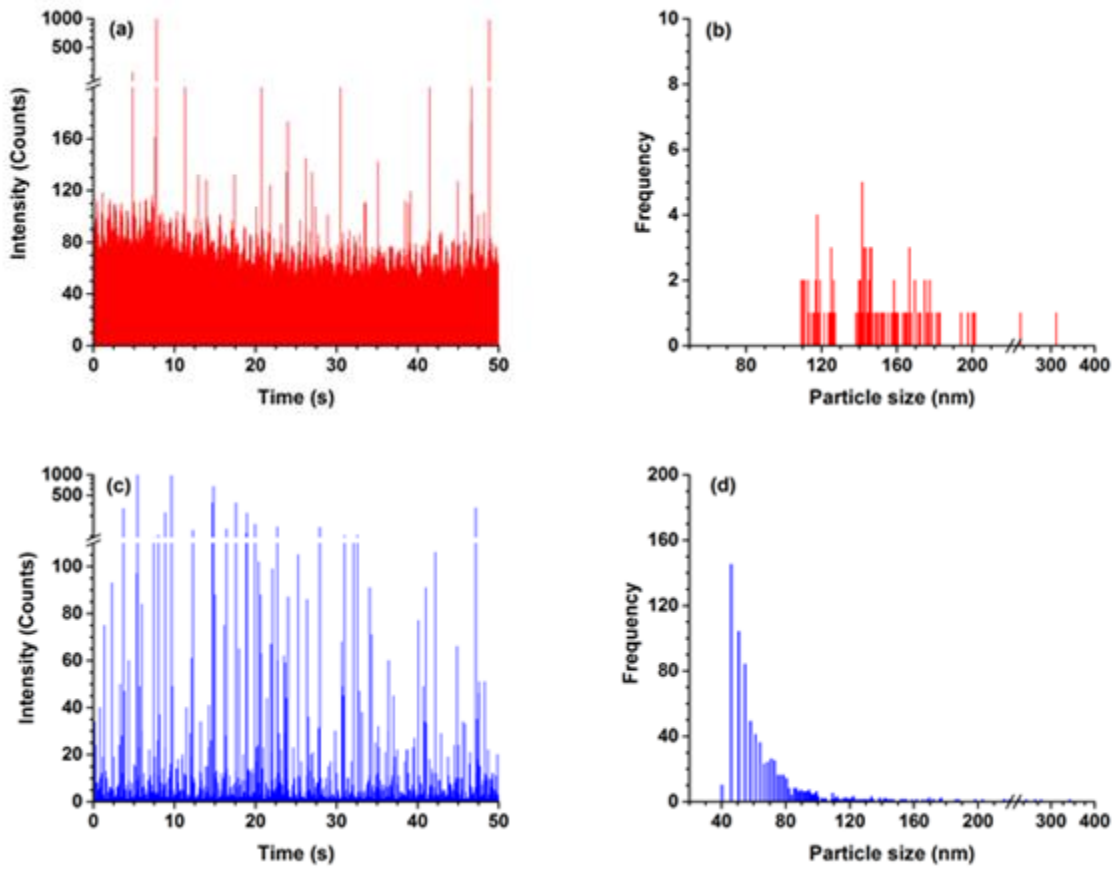

Figure 2. Time resolved signal for a suspension of ZnO nanoparticles (50 nm nominal diameter, 17.7 µg L^{-1} total Zn) in MilliQ water. Signal was acquired by (a) SP-ICPMS and (c) following passage through an online Chelex 100 resin (IEC-SP-ICPMS). Respective size distributions for the data are provided for: (b) SP-ICPMS and (d) IEC-SP-ICPMS.

nZnO in a river water. The presence of major ions at similar concentrations to those generally found in surface waters did not affect the efficiency of the Chelex 100 resin (Figure S3). Natural waters sampled from the *Des Prairies* river (Montreal, Canada; Table S1) were spiked with nZnO nanoparticles. When samples were spiked with less than 10 μg L^{-1} Zn, there were simply not enough nanoparticles to determine particle number or particle diameter, with (i.e. IEC SP-ICPMS) or without (i.e. SP-ICPMS) the Chelex resin (Figure S4). It was only possible to get sufficient particle counts when using higher nZnO concentrations. For example, when the surface water samples were spiked with 36.8 μg L^{-1} Zn of nZnO, a low frequency of large agglomerates were detected (mean: 220.5 nm, mode: 182.5 nm; Figure 3a, 3b) by SP-ICPMS. However, when the Chelex resin was coupled to the SP-ICPMS, it was also possible to identify larger numbers (~10x) of (smaller) nanoparticles (mean: 136.9 nm, mode: 114.1 nm; Figures 3c, 3d). Particle diameters obtained by IEC-SP-ICPMS (Figure 3d) were substantially larger than those determined in MilliQ water (Figure 2d), suggesting that the agglomeration of nZnO or its heterocoaguation with natural colloids may have occurred in the natural water. Similar conclusions could be drawn when the water was spiked with a higher particle concentration (96.3 μg L^{-1} Zn, Table 1 and Figure S5). Clearly, the nZnO was not stable in the surface water- in addition to the observed agglomeration, much of the nZnO dissolved. For example, for the lower nZnO spike, ca. 96.8% of the Zn was attributed to the dissolved fraction.

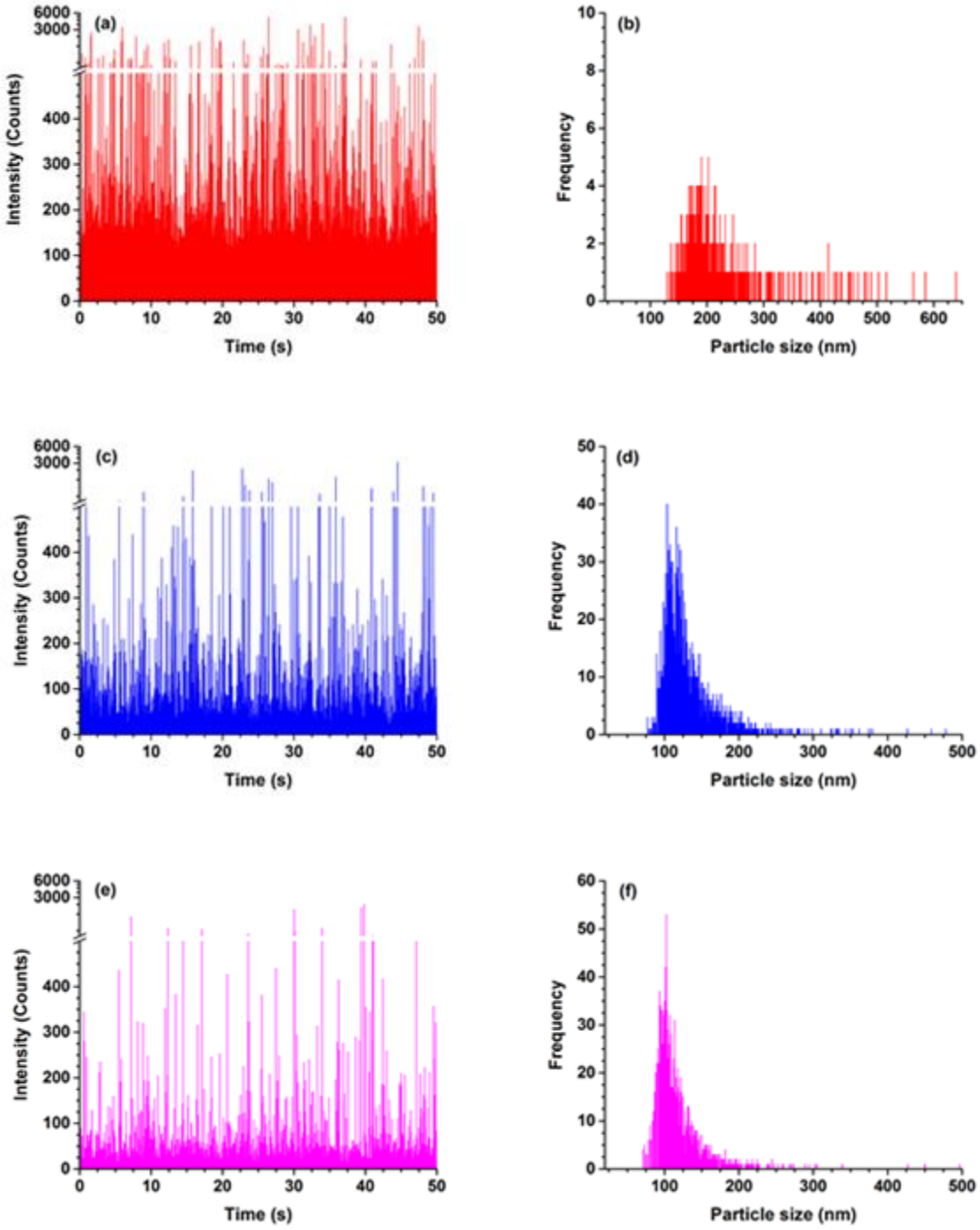

Figure 3. Time resolved signal for a suspension of ZnO nanoparticles (nominal diameter of 50 nm, 36.8 µg L^{-1} total Zn) in the Des Prairies River acquired (a) without the use of a resin (SP-ICPMS); (c) following sample elution through an online Chelex100 and (e) following elution

191 through an online XAD1180N resin. Respective size distributions for the data: (b) SP-ICPMS,
192 (d) IEC-SP-ICPMS and (f) XAD-SP-ICPMS.

193 Unlike the results obtained in MilliQ water, the use of the ion exchange resin did not completely
194 remove all of the dissolved Zn from the background signal (Figure 3c). In natural waters, inorganic
195 (e.g. $ZnSO_4$, $ZnHPO_4$) and organic (e.g. Zn-humic) Zn complexes are likely to be present in
196 addition to free Zn. While the Chelex should remove much of the free Zn and labile Zn complexes,
197 it is unlikely to remove the strong/slowly dissociating complexes in the dissolved fraction. In this
198 case, complex lability is defined with respect to the transit time of the sample through the resin,
199 which is ca. 8 s. Based upon mass balance calculations of the different Zn forms made using SP
200 ICPMS and IEC SP-ICPMS, it was possible to conclude that these non-labile complexes
201 represented less than 10% of the Zn in the surface water (Table 1).

202 Since dissolved Zn may mask small nZnO particles, it was necessary verify that the small
203 background signal observed in Fig. 3c was not responsible for the measured increase in particle
204 size when comparing the natural water with the Milli-Q water. Three lines of reasoning lead us to
205 believe that the increased particle size was real. First, the masking of small particles by the
206 dissolved background should result in decreased particle numbers and decreased particle mass
207 concentrations rather than an increase of particle size. However, when Milli-Q water was spiked
208 with 51 $\mu g\ L^{-1}$ Zn of nZnO, 9.7×10^7 particles per liter were detected (corresponding to a particle
209 mass concentration of 100.2 $ng\ L^{-1}$) whereas the addition of 36 $\mu g\ L^{-1}$ Zn of nZnO to the surface
210 water led to a similar particle number concentration (8.9×10^7 particles L^{-1}) but a much higher
211 average particle intensity and much larger total particle mass (1315.1 $ng\ L^{-1}$, obtained by summing
212 the masses of all of the individual detected particles, Table S2).

213 Second, based upon the signal intensity that was attributed to the dissolved Zn at the exit of the
214 IEC column (Figures 3c; Figure S6), it is possible to estimate a minimum detectable particle size
215 of 32 nm for the samples measured in Milli-Q water and 70 nm for the samples measured in the
216 river water. Given the size detection limit of 70 nm, it is unlikely that the observed high intensity,
217 symmetrical peak centered at 114 nm could be an artifact.

218 Third, under the assumption that the non- labile complexes were mainly Zn bound to humic
219 substances, the SP-ICPMS was also coupled to an XAD1180N resin designed to remove natural
220 organic matter (Figure 3e, 3f). Following passage of the sample through this resin, the background
221 signal of dissolved Zn decreased both with respect to samples run without the columns (SP-
222 ICPMS; Figure 3a) and when compared to samples that were run through the Chelex column (IEC-
223 SP-ICPMS; Figure 3c). Nonetheless, following elution through the XAD, particle diameters
224 decreased only slightly with respect to the Chelex treatment (120.1 ± 5.5 nm (XAD) vs. 136.9 ±
225 3.3 nm). For both resins, particle numbers were substantially higher (~10x) than those measured
226 by SP-ICPMS. In addition, a similar result was obtained when the XAD and Chelex resins were
227 run sequentially- XAD-IEC-SP-ICPMS gave particle sizes that were not significantly different
228 from results determined for the XAD alone. While the use of the XAD allowed us to conclude that
229 particle agglomeration was indeed occurring in the natural water; unlike the observations for the
230 Chelex resin, there was some evidence that the XAD was removing a fraction of the nZnO, likely
231 the larger particles and agglomerates. Given the observed particle losses, the use of this resin was
232 discontinued. Based upon the above reasoning, we concluded that the observed increase in particle
233 size in the river water likely resulted from both increased agglomeration and decreased dissolution
234 of the nZnO, when compared to the Milli-Q water.

Table 1. Speciation of the ZnO nanoparticles in the *Des Prairies* River water and in wastewater effluent (Montreal treatment facility) using single particle ICPMS coupled with a Chelex 100 resin. For each matrix, samples were spiked with two different nZnO concentrations, initially 36.8 or 96.3 μg L^{-1} for surface water and 50.1 or 93.7 μg L^{-1} for wastewater.

	Surface water		**Wastewater effluent**	
Total Zn (μg L^{-1})	36.8	96.3	50.1	93.7
Particle number concentration (10^7 L^{-1})	8.9 ± 0.3	12.8 ± 0.3	0.7 ± 0.05	5.6 ± 0.3
Average Particle Size (nm)	136.9 ± 3.3	170.7 ± 1.7	171.6 ± 4.0	215.0 ± 1.4
Most frequent size (nm)	114.1 ± 1.6	125.5 ± 1.3	153.4 ± 0.6	167.3 ± 0.3
Particulate Zn (%)	3.2 ± 0.1	3.9 ± 0.3	0.6 ± 0.1	3.5 ± 0.3
Zn^{2+} and labile Zn complexes (%)	87.8 ± 0.7	91.0 ± 0.7	51.6 ± 0.8	64.1 ± 1.8
Strong Zn complexes (%)	9.0 ± 0.6	5.1 ± 0.4	47.8 ± 0.7	32.4 ± 1.5

nZnO in a wastewater effluent. The same nZnO nanoparticles (50.1 and 93.7 μg L^{-1} Zn; 50 nm nominal diameter) were added to a wastewater effluent and analyzed by SP-ICPMS and IEC-SP-ICPMS (Table 1; Figures 4, S7). As above, the vast majority of Zn (99.4 ± 0.1%) was initially attributed to the dissolved fraction by SP-ICPMS. Coupling of the Chelex resin lowered the background signal considerably, but it did not substantially increase particle numbers (Figures 4, S7). Indeed, particle numbers were >6x lower than for similar nZnO additions made to the surface water and accounted for only ≤3.5 ± 0.3 % of the total Zn. When compared to the Milli-Q water, a similar nZnO spike (50 μg L^{-1} Zn) gave 14x fewer particles in the wastewater effluent but a higher particle mass concentration (304.3 ng L^{-1} in wastewater; 100.2 ng L^{-1} in Milli-Q). As observed above, nanoparticle diameters were smaller when the Chelex resin was used, however,

the mean particle size (171.6 ± 4.0) was still much larger than the nominal particle size (50 nm) or that observed in the other media (MilliQ water: 65.4 ± 0.5 nm; River water: 136.9 ± 3.3 nm). Furthermore, when the concentration of the nZnO spike was increased from 50.1 to 93.7 µg L^{-1}, both the particle number concentration (8x) and the mean particle size (171 to 215 nm) increased substantially. As shown previously[33] and in the river water, these results suggested that particle dissolution increased with increasing dilution but that in addition to dissolution, a significant fraction of the nZnO losses were probably due to agglomeration/ heterocoagulation, which would be consistent with the much greater hardness of the effluent water as compared to the river water (Table S1). Coupling with the Chelex re-affirmed that, in the wastewater effluent, most (96.5 ± 0.3 %) of the nZnO could be attributed to the dissolved fraction (Figure 4, Table 1).

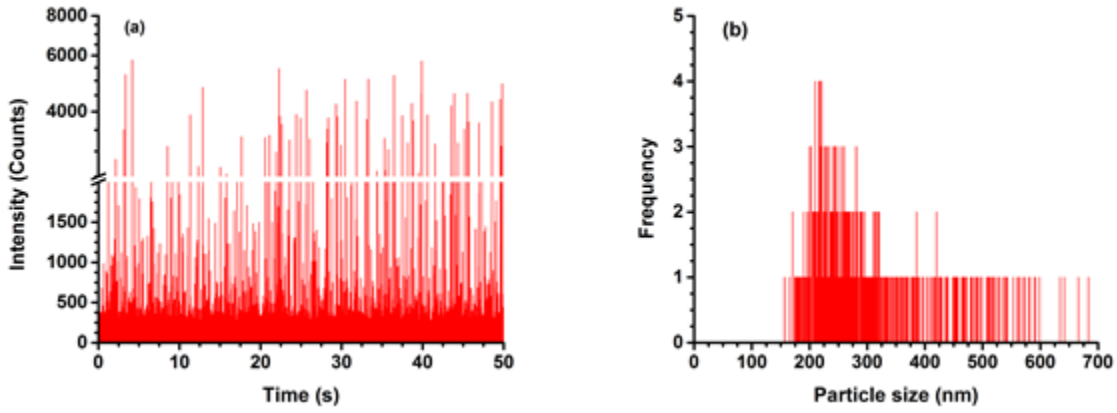

Figure 4. Time resolved signal for a suspension of ZnO nanoparticles (50 nm nominal diameter, 93.7 µg L^{-1} total Zn) in a wastewater effluent (Montreal treatment facility) acquired (a) without passage through a resin (i.e. classical SP-ICPMS) and (c) following passage through an online Chelex 100 resin (IEC-SP-ICPMS). Respective size distributions for the data: (b) SP-ICPMS, (d) IEC-SP-ICPMS.

Zn nanoparticles in unspiked waters. The IEC-SP-ICPMS technique that was developed above was also used for the direct analysis of the natural waters without the addition of a ZnO spike. As above, the majority of Zn was in the dissolved form, however, particulate Zn was also clearly present (Figure 5), where it was found at a very low concentrations of about 5 ng L^{-1} in the surface water and 50 ng L^{-1} in the effluent (Table 2). In all cases, the number of detected particle events was below 100 (sample analysis time of 50 s), which makes the determination of particulate Zn more qualitative than quantitative. Furthermore, given that the composition of the Zn nanoparticles (and thus their density and %Zn) was unknown, it was only possible to estimate particle concentrations and particles sizes (±ca. 50%). For example, based on the assumption that the particle was a spherical zinc oxide, particles would account for 0.1% of the Zn in the river water (mean size of 69 nm, Fig. 5c) and 0.4% of the Zn in the effluent (mean size of 141 nm, Fig. 5d). Based upon these particle numbers, the contributions of the naturally occurring (or incidental) nano-particulate Zn to the spiked waters was not significant (except for the lowest spiked concentrations of nZnO in the wastewater where the incidental nanoparticles would have contributed ca. 16% of the particulate signal).

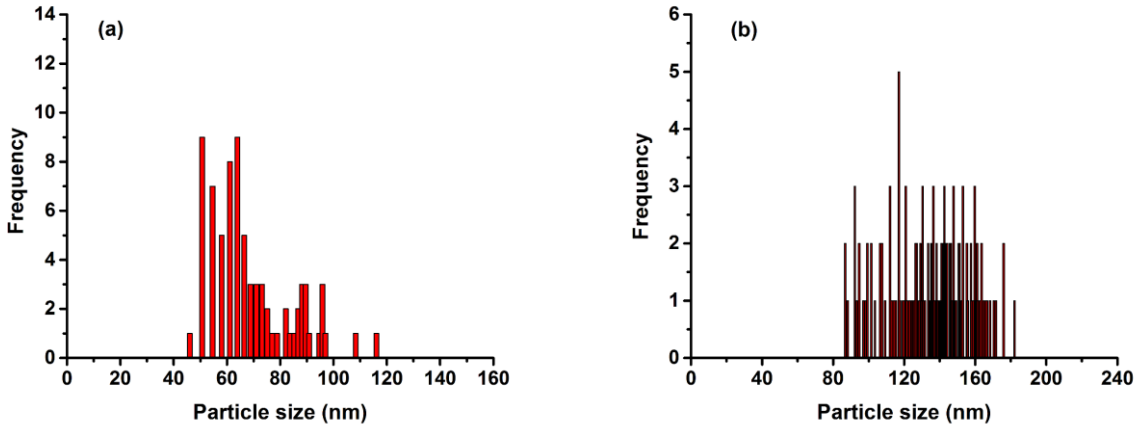

285 **Figure 5.** Particle size distributions for the unspiked samples: (a) the Des Prairies River water and
286 (b) the wastewater effluent (Montreal treatment facility).

287

288 **Table 2.** Concentration of dissolved and particulate Zn (naturally or incidentally occurring
289 nanomaterials) in the Des Prairies River water and the wastewater effluent (Montreal treatment
290 facility) samples. Average particle sizes were estimated as mass equivalent diameters under the
291 assumption of a spherical ZnO.

	Surface water	Effluent waste water
Particulate Zn (µg/L)	0.005 ± 0.001	0.049 ± 0.001
Dissolved Zn (µg/L)	0.636 ± 0.001	12.194 ± 0.001
Average particle size (nm)	69 ± 2	141 ± 6

292

293

294 **Environmental relevance.** To our knowledge, except for imaging techniques and at relatively
295 high concentrations[7, 15,34] this paper represents the first characterization of ppb levels of nZnO in
296 natural water samples. While it was previously impossible to measure nZnO using SP-ICPMS due
297 to their high dissolution, the coupling SP-ICPMS with resins designed to reduce background
298 (dissolved) Zn should allow for their characterization and detection at environmentally relevant

299 concentrations, in both toxicological and environmental media. Using this technique, it should be
300 possible to gain valuable insight not only with respect to the size and concentration of the
301 nanoparticles, but also on their fate in natural matrices.

302

303 **ASSOCIATED CONTENT**

304 Additional data on the equilibration time required for nanoparticle measurements; the possible
305 interaction of ZnO nanoparticles with the Chelex 100 resin; IEC-SP-ICPMS on samples spiked
306 with major cations; the composition of the natural water samples, particle number and particle
307 mass concentrations, size detection limit determinations and additional SP ICPMS results are
308 available in the Supporting Information. This material is available free of charge via the Internet
309 at http://pubs.acs.org.

310 **AUTHOR INFORMATION**

311 **Corresponding Author**

312 *E-mail: kj.wilkinson@umontreal.ca. Tel.: +1 514 343 674. Fax: +1 514 343 7586

313

314 **ACKNOWLEDGMENTS**

315 Funding for this work was provided by the Natural Sciences and Engineering Research Council of
316 Canada, the *Fonds de Recherche du Québec - Nature et Technologies*, the Canadian Water
317 Network and the City of Calgary. Effluent waters were collected from the Montreal WWTP (Flavio
318 Piccapietra, Subhasis Ghoshal, McGill University). The Syngistix nano application software was
319 graciously provided by Perkin Elmer.

REFERENCES

1. Schultz, A. G.; Boyle, D.; Chamot, D.; Ong, K. J.; Wilkinson, K. J.; McGeer, J. C.; Sunahara, G.; Goss, G. G., Aquatic toxicity of manufactured nanomaterials: challenges and recommendations for future toxicity testing. *Environmental Chemistry* **2014,** *11*, (3), 207-226.

2. Lewicka, Z. A.; Yu, W. W.; Oliva, B. L.; Contreras, E. Q.; Colvin, V. L., Photochemical behavior of nanoscale TiO2 and ZnO sunscreen ingredients. *J Photoch Photobio A* **2013,** *263*, 24-33.

3. Shanmugapriya, P.; Thanuja, M. Y.; Anusuya, T.; Pandiyarasan, V., Biologically Prepared ZnO Nanoparticles for Effective Transparent Sunscreen Applications. *Asian J Chem* **2013,** *25*, S255-S257.

4. Hanley, C.; Layne, J.; Punnoose, A.; Reddy, K. M.; Coombs, I.; Coombs, A.; Feris, K.; Wingett, D., Preferential killing of cancer cells and activated human T cells using ZnO nanoparticles. *Nanotechnology* **2008,** *19*, (29).

5. Wahab, R.; Siddiqui, M. A.; Saquib, Q.; Dwivedi, S.; Ahmad, J.; Musarrat, J.; Al-Khedhairy, A. A.; Shin, H. S., ZnO nanoparticles induced oxidative stress and apoptosis in HepG2 and MCF-7 cancer cells and their antibacterial activity. *Colloid Surface B* **2014,** *117*, 267-276.

6. Zheng, W.; Xin, N.; Chi, Z.-H.; Zhao, B.-L.; Zhang, J.; Li, J.-Y.; Wang, Z.-Y., Divalent metal transporter 1 is involved in amyloid precursor protein processing and Abeta generation. *FASEB Journal* **2009,** *23*, (12), 4207-4217, 10 1096/fj 09-135749.

7. Adam, N.; Schmitt, C.; Galceran, J.; Companys, E.; Vakurov, A.; Wallace, R.; Knapen, D.; Blust, R., The chronic toxicity of ZnO nanoparticles and $ZnCl_2$ to Daphnia magna and the use

of different methods to assess nanoparticle aggregation and dissolution. *Nanotoxicology* **2014,** *8*, (7), 709-717.

8. Wong, S. W.; Leung, P. T.; Djurisic, A. B.; Leung, K. M., Toxicities of nano zinc oxide to five marine organisms: influences of aggregate size and ion solubility. *Anal Bioanal Chem* **2010,** *396*, (2), 609-18.

9. Wong, S. W.; Leung, K. M., Temperature-dependent toxicities of nano zinc oxide to marine diatom, amphipod and fish in relation to its aggregation size and ion dissolution. *Nanotoxicology* **2014,** *8 Suppl 1*, 24-35.

10. Miao, A. J.; Zhang, X. Y.; Luo, Z. P.; Chen, C. S.; Chin, W. C.; Santschi, P. H.; Quigg, A., Zinc Oxide Engineered Nanoparticles Dissolution and Toxicity to Marine Phytoplankton. *Environmental Toxicology and Chemistry* **2010,** *29*, (12), 2814-2822.

11. Ma, H. B.; Wallis, L. K.; Diamond, S.; Li, S. B.; Canas-Carrell, J.; Parra, A., Impact of solar UV radiation on toxicity of ZnO nanoparticles through photocatalytic reactive oxygen species (ROS) generation and photo-induced dissolution. *Environmental Pollution* **2014,** *193*, 165-172.

12. Osmond, M. J.; Mccall, M. J., Zinc oxide nanoparticles in modern sunscreens: An analysis of potential exposure and hazard. *Nanotoxicology* **2010,** *4*, (1), 15-41.

13. Waalewijn-Kool, P. L.; Ortiz, M. D.; van Straalen, N. M.; van Gestel, C. A. M., Sorption, dissolution and pH determine the long-term equilibration and toxicity of coated and uncoated ZnO nanoparticles in soil. *Environmental Pollution* **2013,** *178*, 59-64.

14. Franklin, N. M.; Rogers, N. J.; Apte, S. C.; Batley, G. E.; Gadd, G. E.; Casey, P. S., Comparative toxicity of nanoparticulate ZnO, bulk ZnO, and $ZnCl_2$ to a freshwater microalga

(Pseudokirchneriella subcapitata): The importance of particle solubility. *Environ Sci Technol* **2007,** *41*, (24), 8484-8490.

15. Bian, S. W.; Mudunkotuwa, I. A.; Rupasinghe, T.; Grassian, V. H., Aggregation and Dissolution of 4 nm ZnO Nanoparticles in Aqueous Environments: Influence of pH, Ionic Strength, Size, and Adsorption of Humic Acid. *Langmuir* **2011,** *27*, (10), 6059-6068.

16. Han, Y.; Kim, D.; Hwang, G.; Lee, B.; Eom, I.; Kim, P. J.; Tong, M. P.; Kim, H., Aggregation and dissolution of ZnO nanoparticles synthesized by different methods: Influence of ionic strength and humic acid. *Colloid Surface A* **2014,** *451*, 7-15.

17. Hu, C. W., Aggregation and Dissolution of ZnO Nanoparticles in Solutions. *Asian J Chem* **2012,** *24*, (7), 3045-3048.

18. Degueldre, C.; Favarger, P. Y.; Wold, S., Gold colloid analysis by inductively coupled plasma-mass spectrometry in a single particle mode. *Analytica Chimica Acta* **2006,** *555*, (2), 263-268.

19. Degueldre, C.; Favarger, P. Y., Colloid analysis by single particle inductively coupled plasma-mass spectroscopy: a feasibility study. *Colloid Surface A* **2003,** *217*, (1-3), 137-142.

20. Degueldre, C.; Favarger, P. Y.; Rosse, R.; Wold, S., Uranium colloid analysis by single particle inductively coupled plasma-mass spectrometry. *Talanta* **2006,** *68*, (3), 623-628.

21. Laborda, F.; Jimenez-Lamana, J.; Bolea, E.; Castillo, J. R., Selective identification, characterization and determination of dissolved silver(I) and silver nanoparticles based on single particle detection by inductively coupled plasma mass spectrometry. *J Anal Atom Spectrom* **2011,** *26*, (7), 1362-1371.

22. Mitrano, D. M.; Lesher, E. K.; Bednar, A.; Monserud, J.; Higgins, C. P.; Ranville, J. F., Detecting nanoparticulate silver using single-particle inductively coupled plasma–mass spectrometry. *Environmental Toxicology and Chemistry* **2012,** *31*, (1), 115-121.

23. Tuoriniemi, J.; Cornelis, G.; Hassellov, M., Size Discrimination and Detection Capabilities of Single-Particle ICPMS for Environmental Analysis of Silver Nanoparticles. *Anal Chem* **2012,** *84*, (9), 3965-3972.

24. Allabashi, R.; Stach, W.; de la Escosura-Muniz, A.; Liste-Calleja, L.; Merkoci, A., ICP-MS: a powerful technique for quantitative determination of gold nanoparticles without previous dissolving. *J Nanopart Res* **2009,** *11*, (8), 2003-2011.

25. Liu, J. Y.; Murphy, K. E.; MacCuspie, R. I.; Winchester, M. R., Capabilities of Single Particle Inductively Coupled Plasma Mass Spectrometry for the Size Measurement of Nanoparticles: A Case Study on Gold Nanoparticles. *Anal Chem* **2014,** *86*, (7), 3405-3414.

26. Loeschner, K.; Brabrand, M. S. J.; Sloth, J. J.; Larsen, E. H., Use of alkaline or enzymatic sample pretreatment prior to characterization of gold nanoparticles in animal tissue by single-particle ICPMS. *Analytical and Bioanalytical Chemistry* **2014,** *406*, (16), 3845-3851.

27. Linsinger, T. P. J.; Peters, R.; Weigel, S., International interlaboratory study for sizing and quantification of Ag nanoparticles in food simulants by single-particle ICPMS. *Analytical and Bioanalytical Chemistry* **2014,** *406*, (16), 3835-3843.

28. Telgmann, L.; Metcalfe, C. D.; Hintelmann, H., Rapid size characterization of silver nanoparticles by single particle ICP-MS and isotope dilution. *J Anal Atom Spectrom* **2014,** *29*, (7), 1265-1272.

29. Peters, R. J.; Rivera, Z. H.; van Bemmel, G.; Marvin, H. J.; Weigel, S.; Bouwmeester, H., Development and validation of single particle ICP-MS for sizing and quantitative determination of nano-silver in chicken meat. *Anal Bioanal Chem* **2014,** *406*, (16), 3875-85.

30. Reed, R. B.; Higgins, C. P.; Westerhoff, P.; Tadjiki, S.; Ranville, J. F., Overcoming challenges in analysis of polydisperse metal-containing nanoparticles by single particle inductively coupled plasma mass spectrometry. *J Anal Atom Spectrom* **2012,** *27*, (7), 1093-1100.

31. Hadioui, M.; Peyrot, C.; Wilkinson, K. J., Improvements to Single Particle ICPMS by the Online Coupling of Ion Exchange Resins. *Anal Chem* **2014,** *86*, (10), 4668-4674.

32. Hineman, A.; Stephan, C., Effect of dwell time on single particle inductively coupled plasma mass spectrometry data acquisition quality. *J Anal Atom Spectrom* **2014,** *29*, (7), 1252-1257.

33. Merdzan, V.; Domingos, R. F.; Monteiro, C. E.; Hadioui, M.; Wilkinson, K. J., The effects of different coatings on zinc oxide nanoparticles and their influence on dissolution and bioaccumulation by the green alga, C. reinhardtii. *Science of the Total Environment* **2014,** *488*, 316-324.

34. Domingos, R.F., Baalousha, M.A., Ju-Nam, Y., Reid, M., Tufenkji, N., Lead, J.R., Leppard, G.G. and K.J. Wilkinson. Characterizing manufactured nanoparticles in the environment - multimethod determination of particle sizes. *Environ. Sci. Technol*. **2009**, *43,* 7277-7284.